Proc. Asia-Pacific Conf. on Semiconducting Silicides and Related Materials 2016
JJAP Conf. Proc. **5**, 011202 (2017) https://doi.org/10.7567/JJAPCP.5.011202

Preferred Orientation of $BaSi_2$ Thin Films Fabricated by Thermal Evaporation

Kosuke O. Hara[1], Cham Thi Trinh[2,3], Yoshihiko Nakagawa[2], Yasuyoshi Kurokawa[2], Keisuke Arimoto[1], Junji Yamanaka[1], Kiyokazu Nakagawa[1], and Noritaka Usami[2]

[1]*Center for Crystal Science and Technology, University of Yamanashi, Yamanashi 400-8511, Japan*
[2]*Graduate School of Engineering, Nagoya University, Nagoya 464-8603, Japan*
[3]*Present address: Institut Silizium-Photovoltaik, Helmholtz-Zentrum Berlin für Materialien und Energie, D-12489 Berlin, Germany*

E-mail: khara@yamanashi.ac.jp

(Received August 30, 2016)

Thermal evaporation is a simple and high-speed method to grow a $BaSi_2$ thin film, which is an emerging candidate for an absorber-layer material of thin-film solar cells. In this study, we have investigated the preferred orientation of $BaSi_2$ films grown at substrate temperatures of 600–700 °C by thermal evaporation using X-ray diffraction. 2θ–ω scans show that peaks derived from (100) orientation grow steadily with increasing substrate temperature. By X-ray pole figure analysis, the (100)-oriented crystals are proven to be epitaxially grown on Si(100) with two variants. The reason of epitaxial growth is discussed from the epitaxial temperature.

1. Introduction

Orthorhombic $BaSi_2$ is an attractive material for thin-film solar cell applications because of the abundance of constituent elements in the earth's crust as well as excellent properties such as a suitable band gap of 1.1–1.3 eV [1–4], high absorption coefficients [3], and long minority-carrier lifetime (up to 11 μs [5]) and diffusion length (10 μm [6]). Control of the carrier type and conductivity is possible by impurity doping [7–9], which enables one to design various device structures. Recently, a high power conversion efficiency reaching 9.0 % has been reported by using a p-type $BaSi_2$/n-type Si heterojunction structure [10].

Fundamental properties and device applications of $BaSi_2$ have been studied mainly using (100)-oriented epitaxial films grown by molecular beam epitaxy (MBE) on Si substrates [11,12]. For practical applications, however, a more simple and high-speed film growth method is preferable. We are hence developing a thermal evaporation technique using a $BaSi_2$ source. So far, single-phase $BaSi_2$ films have been formed on various substrates such as Si [13–17], glass [4,14], and CaF_2 [18]. On single-crystal Si substrates, the $BaSi_2$ films have been proven to be oriented polycrystals [13]. The preferred orientation is, however, not decided. For further understanding of the film growth mechanism, the information on preferred orientation is important. In this study, therefore, we investigated the crystal orientation of evaporated $BaSi_2$ films, especially focusing on the effects of substrate temperature (T_{sub}). It is shown that partial epitaxial growth with (100) orientation is possible by the simple evaporation technique at high T_{sub}'s, which suggests that the (100) orientation of $BaSi_2$ is preferable on Si(100) from an energetic viewpoint.

2. Experimental methods

Commercial $BaSi_2$ lumps (99 % in purity, Kojundo Chemical Lab.) were used as a source material of evaporation after grinding. They were loaded onto a tungsten boat in the vacuum chamber and were melted by resistive heating of the boat. After complete melting of $BaSi_2$, the shutter was opened and the heating current was raised for film deposition. The substrate used was p-type Si(100) wafer with a resistivity of over 1000 Ω·cm. T_{sub} was varied in a range of 600–700 °C. Base pressure of the chamber was below 1×10^{-3} Pa. Produced films were characterized by scanning electron microscopy (SEM; JEOL JSM-6500F and Hitachi TM3030), 2θ–ω X-ray diffraction analysis (XRD; Bruker Discover D8) with Cu Kα radiation, and X-ray pole figure analysis with an area detector (Bruker Discover D8).

3. Results and discussion

The morphology of the produced films observed by SEM is shown in Fig. 1. At $T_{sub} = 600$ °C,

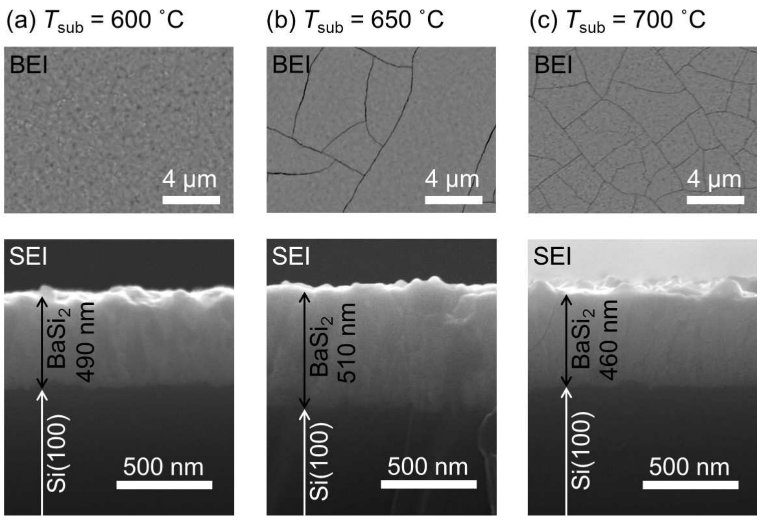

Fig. 1. SEM pictures of evaporated $BaSi_2$ films grown at $T_{sub} = 600$–700 °C. Plan-view pictures are backscattered electron images (BEI) taken by TM3030 while cross-sectional ones are secondary electron images (SEI) by JSM6500F.

a dense film without cracks is formed. On the other hand, at higher T_{sub}'s, cracks appear on the surface. The density of cracks is higher for $T_{sub} = 700$ °C than 650 °C, indicating that cracking is because of thermal stress, as has been observed in previous studies [4, 19]. The $BaSi_2$ film thicknesses determined from the cross-sectional pictures are in a range of 460–510 nm.

Figure 2 shows 2θ–ω XRD patterns of evaporated $BaSi_2$ films. All peaks are attributed to orthorhombic $BaSi_2$ phase and Si substrate, assuring that the film consists of $BaSi_2$. It is clearly observed that the relative peak intensity of $BaSi_2$ is significantly different from the simulated powder pattern, which shows that the $BaSi_2$ films are preferentially oriented.

At $T_{sub} = 600$ °C, 301 or 004 diffraction is relatively strong. Since 002 diffraction at $2\theta = 15.4°$ was not observed, 301 is more plausible than 004, corresponding to the (301) preferential orientation. At $T_{sub} = 650$ °C, 301 peak becomes weak. Instead, 222 or 123 diffraction is strongest. Because 111 or 102 diffraction is also strong, preferential orientation

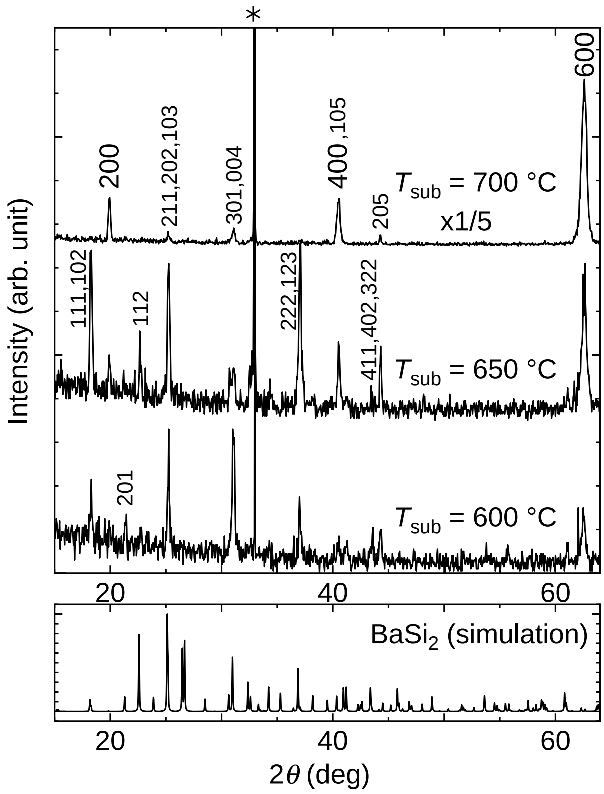

Fig. 2. 2θ–ω XRD patterns of evaporated $BaSi_2$ films together with theoretical powder pattern of $BaSi_2$. The asterisk symbol denotes the peak from Si(100) substrate. Three digit numbers are diffraction indices for $BaSi_2$.

is probably (111) and the strong diffractions are 111 and 222. By further increasing T_{sub} to 700 °C, preferential orientation changes again. The 111 and 222 diffractions become invisible. The strongest peak is 600 diffraction at this temperature. The 200 and 400 diffractions are also strong while the other diffractions are very weak, indicating that almost all $BaSi_2$ crystals are (100)-oriented at $T_{sub} = 700$ °C. From the present experimental results, it is difficult to find out the reason why (301) and (111) orientations are preferred at $T_{sub} = 600$ and 650 °C, respectively, because any straightforward trends of diffraction intensity are not observed. On the other hand, the diffraction intensity of $h00$ increases steadily with increasing T_{sub}. This result suggests that the (100) orientation of $BaSi_2$ is more preferable on the Si(100) surface from an energetic viewpoint. Other orientations may have been kinetically stabilized at low temperatures.

Since the (100) orientation of $BaSi_2$ on Si(100) surface is similar to $BaSi_2$ films grown on Si(100) by MBE, the evaporated $BaSi_2$ film at $T_{sub} = 700$ °C may have also grown epitaxially on Si(100). To determine the crystal orientation of evaporated $BaSi_2$ films, therefore, we also performed X-ray pole figure measurement. Each two-dimensional (2D) XRD pattern was taken by scanning the ϕ axis with a 2θ angle of the area detector fixed at 31.1°, which corresponds to the 301 diffraction. The pole figures obtained by integrating the 2D patterns are shown in Fig. 3. In this figure, the transverse (TD) and rolling directions (RD) correspond to the Si<011> directions. The evaporated film grown at $T_{sub} = 700$ °C shows two sets of four spots with intervals of 90° [Fig. 3(a)]. The inner set corresponds to the 301 diffraction while

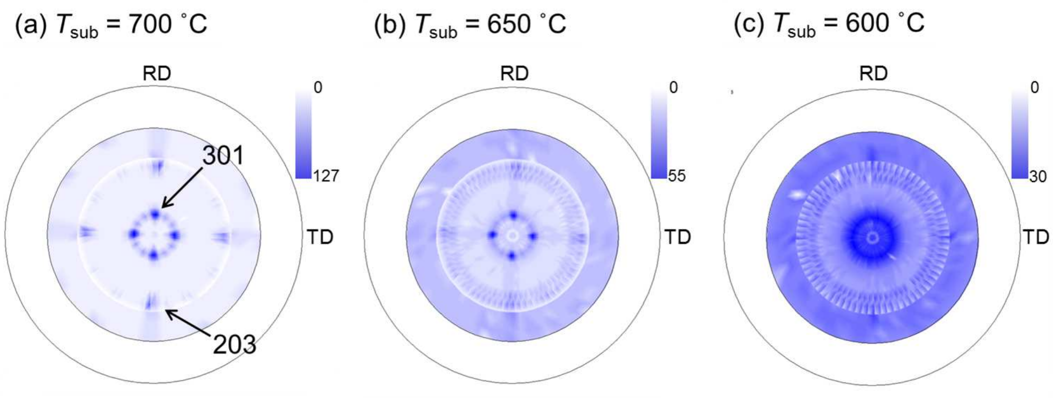

Fig. 3. X-ray pole figures of evaporated $BaSi_2$ films grown at $T_{sub} = 600–700$ °C.

the outer one is 203, the 2θ angle of which is 30.7°. This pole figure clearly shows that the evaporated film was grown epitaxially on Si(100) with two epitaxial variants. The orientation relationships are $BaSi_2$[010]//Si[011] and $BaSi_2$[001]//Si[011] with $BaSi_2$(100)//Si(100) for two variants. These relationships are the same as those of an epitaxial $BaSi_2$ film grown on Si(100) by MBE [12].

Similar two sets of spots are observed from the evaporated film grown at 650 °C. The intensity of spots are, however, weaker than 700 °C. By considering the 2θ–ω scan and pole figure results, a part of this film is epitaxially grown with the same relationship at 700 °C, while the rest consists of polycrystals with (111) preferential orientation. At a lower temperature of 600 °C, strong spots are not observed. Instead, signals are relatively strong around the normal direction, which agrees with strong 301 diffraction in the 2θ–ω pattern. The evaporated film grown at 600 °C, therefore, has preferred orientation of (301) without epitaxy.

It is known that epitaxial growth occurs with evaporation methods when the growth temperature exceeds a minimum temperature (epitaxial temperature), which has been reported for various materials including metals and semiconductors grown on metal, semiconductor, oxide, and halide substrates [20–22]. From the present results, the epitaxial temperature of $BaSi_2$ on Si(100) is speculated to be above 650 °C when grown by thermal evaporation. Although the epitaxial temperature of MBE-grown $BaSi_2$ on Si(100) is not reported, it is known for Si(111) substrate. With a reactively-deposited template layer, epitaxial growth is reported in a wide T_{sub} range of 450–700 °C [11]. On the other hand, without a template layer, epitaxial growth occurs below 650 °C [11]. This significant difference of epitaxial temperatures between thermal evaporation and MBE is presumably due to a different crystal growth mechanism. The existence of a template layer formed by the reactive deposition epitaxy [23] also significantly influences the epitaxial temperature. During thermal evaporation, Ba-rich vapor is supplied to the substrate at the initial stage. The initial $BaSi_2$ layer formed by the reaction between Ba-rich vapor and Si substrate may serve similarly as the template layer in MBE, which may be one of the reasons of epitaxial growth during thermal evaporation at high T_{sub}. At low T_{sub}, thermal diffusion may not be enough to reach thermal equilibrium due to high deposition rates of thermal evaporation, which might account for other kinetically-stabilized preferred orientations.

4. Conclusions

In this study, we have investigated the crystal orientation of $BaSi_2$ thin films grown by thermal evaporation. It has been found by 2θ–ω XRD and pole figure analyses that (100)-oriented epitaxial growth of $BaSi_2$ is possible on Si(100) by increasing T_{sub} to 700 °C. The epitaxial relationship of $BaSi_2$(100)/Si(100) with two epitaxial variants is the same for thermal evaporation and MBE. A significant difference of epitaxial temperatures between thermal evaporation and MBE is probably due to different crystal growth mechanisms.

Acknowledgment

This work was partly supported by JSPS KAKENHI Grant Number 15K18040 and the Murata Science Foundation.

References

[1] T. Nakamura, T. Suemasu, K. Takakura, F. Hasegawa, A. Wakahara and M. Imai, Appl. Phys. Lett. **81**, 1032 (2002).
[2] S. Kishino, T. Imai, T. Iida, Y. Nakaishi, M. Shinada, Y. Takanashi and N. Hamada, J. Alloys Compd. **428**, 22 (2007).
[3] K. Toh, T. Saito and T. Suemasu, Jpn. J. Appl. Phys. **50**, 068001 (2011).
[4] K. O. Hara, Y. Nakagawa, T. Suemasu and N. Usami, Jpn. J. Appl. Phys. **54**, 07JE02 (2015).
[5] K. O. Hara, N. Usami, K. Nakamura, R. Takabe, M. Baba, K. Toko and T. Suemasu, Appl. Phys. Express **6**, 112302 (2013).
[6] M. Baba, K. Toh, K. Toko, N. Saito, N. Yoshizawa, K. Jiptner, T. Sekiguchi, K. O. Hara, N. Usami and T. Suemasu, J. Cryst. Growth **348**, 75 (2012).
[7] M. Kobayashi, Y. Matsumoto, Y. Ichikawa, D. Tsukada and T. Suemasu, Appl. Phys. Express **1**, 051403 (2008).
[8] M. A. Khan, K. Hara, W. Du, M. Baba, K. Nakamura, M. Suzuno, K. Toko, N. Usami and T. Suemasu, Appl. Phys. Lett. **102**, 112107 (2013).
[9] K. O. Hara, W. Du, K. Arimoto, J. Yamanaka, K. Nakagawa, K. Toko, T. Suemasu and N. Usami, Thin Solid Films **603**, 218 (2016).
[10] D. Tsukahara, S. Yachi, H. Takeuchi, R. Takabe, W. Du, M. Baba, Y. Li, K. Toko, N. Usami and T. Suemasu, Appl. Phys. Lett. **108**, 152101 (2016).
[11] Y. Inomata, T. Nakamura, T. Suemasu and F. Hasegawa, Jpn. J. Appl. Phys. **43**, L478 (2004).
[12] K. Toh, K. O. Hara, N. Usami, N. Saito, N. Yoshizawa, K. Toko and T. Suemasu, J. Cryst. Growth **345**, 16 (2012).
[13] Y. Nakagawa, K. O. Hara, T. Suemasu and N. Usami, Jpn. J. Appl. Phys. **54**, 08KC03 (2015).
[14] K. O. Hara, K. Nakagawa, T. Suemasu and N. Usami, Procedia Eng. **141**, 27 (2016).
[15] Y. Nakagawa, K. O. Hara, T. Suemasu and N. Usami, Procedia Eng. **141**, 23 (2016).
[16] K. O. Hara, C. T. Trinh, K. Arimoto, J. Yamanaka, K. Nakagawa, Y. Kurokawa, T. Suemasu and N. Usami, J. Appl. Phys. **120**, 045103 (2016).
[17] C. T. Trinh, Y. Nakagawa, K. O. Hara, R. Takabe, T. Suemasu and N. Usami, Mater. Res. Express **3**, 076204 (2016).
[18] K. O. Hara, J. Yamanaka, K. Arimoto, K. Nakagawa, T. Suemasu and N. Usami, Thin Solid Films **595A**, 68 (2015).
[19] K. O. Hara, N. Usami, K. Nakamura, R. Takabe, M. Baba, K. Toko and T. Suemasu, Phys. Status Solidi C **10**, 1677 (2013).
[20] E. Krikorian and R. J. Sneed, J. Appl. Pnys. **37**, 3665 (1966).
[21] T. Itoh, S. Hasegawa and N. Kaminaka, J. Appl. Phys. **40**, 2597 (1969).
[22] E. Grünbaum, Vacuum **24**, 153 (1974).
[23] Y. Inomata, T. Nakamura, T. Suemasu and F. Hasegawa, Jpn. J. Appl. Phys. **43**, 4155 (2004).